Temperature dependence of Dyakonov-Perel spin relaxation in zinc-blende semiconductor quantum structures

J. Kainz* and U. Rössler

Institut für Theoretische Physik, Universität Regensburg, 93040 Regensburg, Germany

R. Winkler

Institut für Festkörperphysik, Universität Hannover, Appelstrasse 2, 30167 Hannover, Germany

The Dyakonov-Perel mechanism, intimately related to the spin splitting of the electronic states, usually dominates the spin relaxation in zinc-blende semiconductor quantum structures. Previously it has been formulated for the two limiting cases of low and high temperatures. Here we extend the theory to give an accurate description of the intermediate regime which is often relevant for room temperature experiments. Employing the self-consistent multiband envelope function approach, we determine the spin splitting of electron subbands in n-(001) zinc-blende semiconductor quantum structures. Using these results we calculate spin relaxation rates as a function of temperature and obtain excellent agreement with experimental data.

I. INTRODUCTION

In the context of spintronic devices, the spin degree of freedom has recently attracted considerable interest.[1–5] Long spin-relaxation times are crucial for the operation of such devices. Therefore a quantitative understanding is required of how spin relaxation depends on the system parameters and operating conditions. It is generally accepted[6] that in bulk semiconductors with a zinc-blende structure and in quantum well (QW) structures based on these materials the electronic spin relaxation is dominated by the Dyakonov-Perel[6–14] (DP) and the Bir-Aronov-Pikus[15] mechanisms. In the present work, we consider n-doped two-dimensional (2D) systems, where the DP mechanism becomes dominant. This mechanism is intimately related to the spin splitting of the electronic subbands in systems lacking inversion symmetry.[9,10] The spin splitting can result from the inversion asymmetry of the bulk crystal structure [bulk inversion asymmetry (BIA)][16] and from the inversion asymmetry of the QW structure [structure inversion asymmetry (SIA)].[17] The interplay of BIA and SIA in asymmetrically doped QWs gives rise to anisotropic spin relaxation[10–13] for spins aligned along different crystallographic directions.

Previously, the DP theory has been formulated for the limiting cases of low and high temperatures (i.e., for degenerate and nondegenerate electron systems).[8–10,13] Here we extend the theory to arbitrary temperatures in between these limiting cases. Our calculations show that often room temperature falls into this intermediate regime. Therefore our findings are particularly important for spintronic devices working at room temperature.[18] We discuss the details of the temperature dependence and address the influence of various momentum scattering mechanisms. The temperature dependence of the spin relaxation is strongly affected by the temperature dependence of the momentum scattering mechanisms, which are ruled by different power laws in the electron energy.

We present accurate calculations of the temperature-dependent spin-relaxation rates assuming realistic system parameters. The spin splittings are obtained from self-consistent calculations in the multiband envelope-function approximation (EFA).[19] We compare the calculated results with experimental data for symmetric n-doped (001)-grown GaAs/AlGaAs QWs measured by Terauchi *et al.*[20] and Ohno *et al.*[21] Theory and experiment agree very well. Our calculations show that the anisotropy of the spin relaxation persists up to room temperature.

II. DYAKONOV-PEREL MECHANISM AND SPIN SPLITTING

In a single band approach, the DP spin relaxation is based on the time evolution of the electron spin polarization

$$S = \langle \mathrm{Tr}(\varrho_k \boldsymbol{\sigma}) \rangle = \sum_k \mathrm{Tr}(\varrho_k \boldsymbol{\sigma}), \tag{1}$$

where k is the electron wave vector, $\boldsymbol{\sigma}$ is the vector of Pauli spin matrices, and ϱ_k is the 2×2 electron spin-density matrix. The dynamics of S is ruled by a Bloch-like equation containing the spin-orbit coupling

$$H_{\mathrm{so}} = \frac{\hbar}{2} \boldsymbol{\sigma} \cdot \boldsymbol{\Omega}(\boldsymbol{k}). \tag{2}$$

The spin-orbit coupling (2) is similar to a Zeeman term, but $\boldsymbol{\Omega}(\boldsymbol{k})$ is an effective magnetic field that depends on the underlying material, on the geometry of the device, and on the electron wave vector $\boldsymbol{k}$. The vector $\mathrm{Tr}(\varrho_k \boldsymbol{\sigma})$ precesses about $\boldsymbol{\Omega}(\boldsymbol{k})$ which results in spin relaxation. However, (spin independent) momentum scattering of the electrons with, e.g., phonons, (nonmagnetic) impurities or other electrons[22,23] changes $\boldsymbol{k}$ and thus the direction and magnitude of $\boldsymbol{\Omega}(\boldsymbol{k})$ felt by the electrons. Therefore frequent scattering [on the time scale of $|\boldsymbol{\Omega}(\boldsymbol{k})|^{-1}$] suppresses the precession and the spin relaxation. This is the motional narrowing that is typical for the DP mechanism,[8] according to which the spin relaxation rate $\tau_s^{-1} \propto \tau_p$. Here τ_p is the momentum scattering time.

Due to time reversal invariance we have $\mathbf{\Omega}(0)=0$, while for finite $\mathbf{k}$ the spin-orbit coupling H_{so} causes a spin splitting $\hbar|\mathbf{\Omega}(\mathbf{k})|$ of the electron states. In this article we focus on quasi-2D systems grown on a (001) surface and made from semiconductors with a zinc-blende structure. In leading order, the effective field in these systems reads

$$\mathbf{\Omega}(\mathbf{k}_\parallel) = \frac{2\gamma}{\hbar}\begin{pmatrix} k_x(k_y^2 - \langle k_z^2\rangle) \\ k_y(\langle k_z^2\rangle - k_x^2) \\ 0 \end{pmatrix} + \frac{2\alpha}{\hbar}\begin{pmatrix} k_y \\ -k_x \\ 0 \end{pmatrix}. \tag{3}$$

The first term characterizes the BIA spin splitting of the electron states. It is called the Dresselhaus or k^3 term.[16,24] It exists already in bulk semiconductors with broken inversion symmetry. In quasi-2D systems only the in-plane wave vector $\mathbf{k}_\parallel = (k_x, k_y, 0)$ is a continuous variable. In first order perturbation theory, the wave vector components k_z and powers thereof are replaced by expectation values with respect to the subband wave functions.

In asymmetric QWs, SIA gives rise to the second term in Eq. (3) which is frequently called the Rashba term.[17] The coefficients γ and α depend on the underlying semiconductor bulk material; but α depends also on the asymmetry of the QW in growth direction.

Within the DP mechanism the relaxation of the components of $\mathbf{S}$ is ruled by[8]

$$\frac{\partial}{\partial t}S_i = -\frac{1}{\tau_i}S_i, \tag{4}$$

where $i = z, +, -$ corresponds to the components of $\mathbf{S}$ along [001], [110], and [$\bar{1}$10], and we have $S_\pm = 1/\sqrt{2}(S_x \pm S_y)$. The spin-relaxation rates are[13]

$$\frac{1}{\tau_z} = \frac{4}{\hbar^2}\hat{I}\tau_1\left[k_\parallel^2(\alpha^2 + \gamma^2\langle k_z^2\rangle^2) - k_\parallel^4\frac{\gamma^2\langle k_z^2\rangle}{2} + k_\parallel^6\gamma^2\frac{1+\tau_3/\tau_1}{16}\right], \tag{5a}$$

$$\frac{1}{\tau_\pm} = \frac{2}{\hbar^2}\hat{I}\tau_1\left[k_\parallel^2(\pm\alpha - \gamma\langle k_z^2\rangle)^2 + k_\parallel^4\frac{\gamma}{2}(\pm\alpha - \gamma\langle k_z^2\rangle)\right.$$
$$\left. + k_\parallel^6\gamma^2\frac{1+\tau_3/\tau_1}{16}\right]. \tag{5b}$$

The symbol $\hat{I}$ denotes an integral operator which is acting on functions $f(\mathbf{k}_\parallel)$ according to

$$\hat{I}f = \frac{1}{\int(F_+ - F_-)d^2k_\parallel}\int(F_+ - F_-)f(\mathbf{k}_\parallel)d^2k_\parallel, \tag{6}$$

where

$$F_\pm = \frac{1}{1 + e^{\beta[E(\mathbf{k}_\parallel) - \mu_\pm]}}, \tag{7}$$

is the Fermi distribution function, $\beta = 1/(k_B T)$, and μ_+ and μ_- are the chemical potentials for up and down spins, respectively. In Eq. (5), the relaxation times τ_1 and τ_3 are given by

$$\frac{1}{\tau_n(\mathbf{k}_\parallel)} = \sum_{\mathbf{k}'_\parallel} W(\mathbf{k}_\parallel, \mathbf{k}'_\parallel)[1 - \cos(n\theta)], \tag{8}$$

where $W(\mathbf{k}_\parallel, \mathbf{k}'_\parallel)$ is the momentum scattering rate between the states with wave vectors $\mathbf{k}_\parallel$ and $\mathbf{k}'_\parallel$, calculated according to Fermi's golden rule.[25] The symbol θ denotes the angle between $\mathbf{k}_\parallel$ and $\mathbf{k}'_\parallel$.

III. DYAKONOV-PEREL THEORY FOR ARBITRARY TEMPERATURE

In the following we use the effective mass approximation

$$E(\mathbf{k}) = k^2/\zeta, \tag{9}$$

where $\zeta = 2m^*/\hbar^2$, so that we can switch from $\mathbf{k}_\parallel$ to E as the integration variable in Eq. (5). Assuming a sufficiently small[26] difference $\Delta\mu = \mu_+ - \mu_-$, we have $F_+ - F_- \approx -\Delta\mu(\partial F_0/\partial E)$ and $\hat{I}$ can be simplified to

$$\hat{I}f \approx \frac{1}{\int\left(\frac{-\partial F_0}{\partial E}\right)dE}\int dE\left(\frac{-\partial F_0}{\partial E}\right)f(E) \tag{10}$$

independent of $\Delta\mu$. Here

$$F_0 = \frac{1}{1 + e^{\beta[E-\mu_0]}} \tag{11}$$

is the equilibrium Fermi distribution with the temperature-dependent chemical potential μ_0. For a 2D system with parabolic energy dispersion (9) the chemical potential μ_0 can be exactly evaluated giving

$$\mu_0 = \frac{1}{\beta}\ln(e^{E_F\beta} - 1), \tag{12}$$

where E_F is the Fermi energy at temperature $T=0$.

To proceed further, we must specify the scattering times τ_1 and τ_3. Most scattering mechanisms[25,27] have a power-law dependence of τ_1 and τ_3 on the energy E with the same characteristic exponent ν

$$\tau_1 = \Xi E^\nu, \quad \tau_3 \propto E^\nu, \tag{13}$$

where Ξ is a constant independent of E. (Note, however, that in general Ξ depends on T.) Then, τ_3/τ_1 is a constant describing the angular scattering characteristics of the scattering mechanism (see Appendix 2).

A short calculation yields

$$\hat{I}E^n = \frac{J_n(\beta\mu_0)}{\beta^n(1 - e^{-E_F\beta})}, \tag{14}$$

where

$$J_n(z) = \int_0^\infty \frac{x^n}{4\cosh^2\left(\frac{x-z}{2}\right)}dx. \tag{15}$$

In particular, we find using Eq. (12)
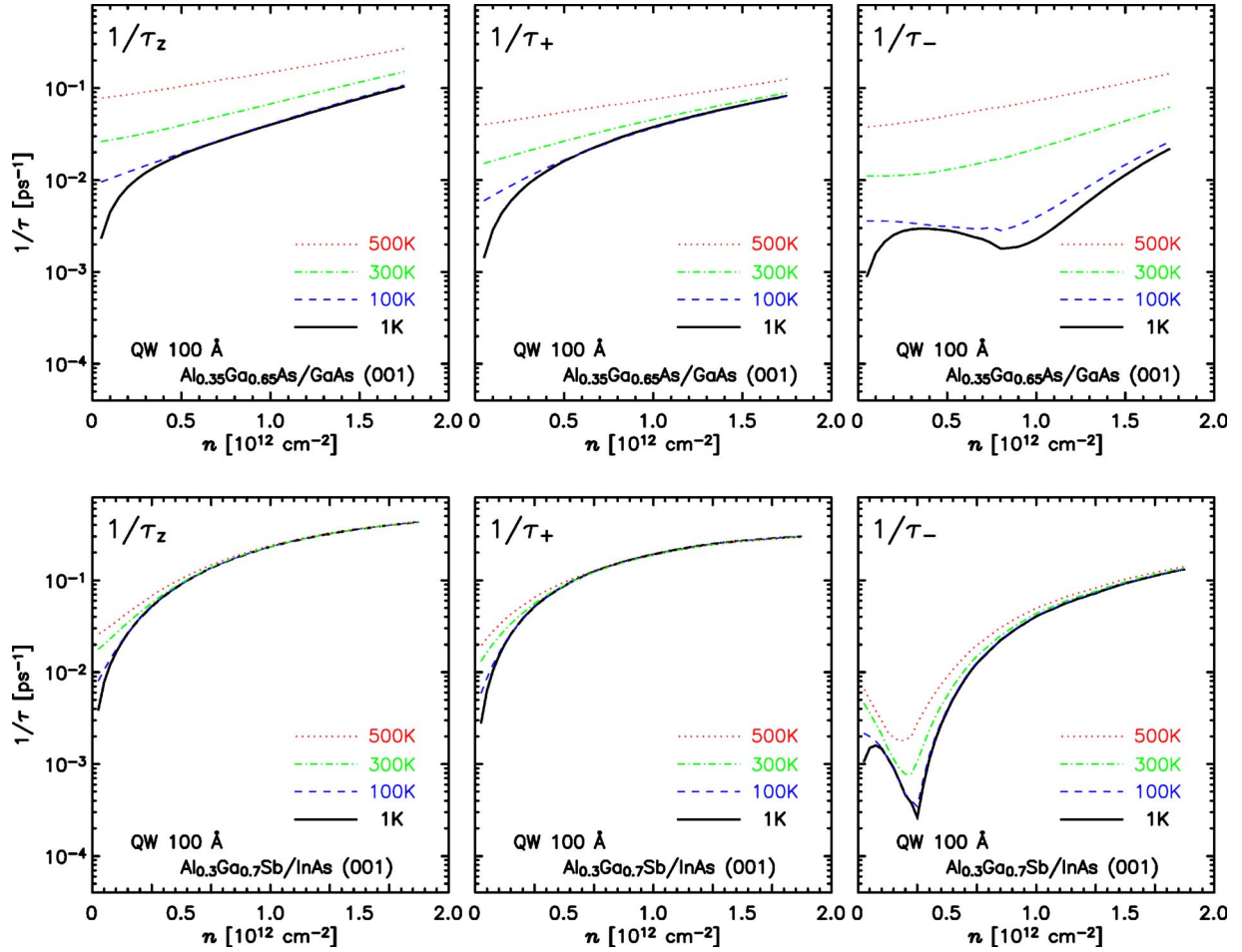
$$J_0(\beta\mu_0) = 1 - e^{-E_F\beta}, \tag{16a}$$

FIG. 1. (Color online) Spin-relaxation rates τ_z^{-1} and $\tau_\pm^{-1}$ as a function of carrier density n and for different temperatures T in asymmetric (001) grown $Al_{0.35}Ga_{0.65}As/GaAs$-QWs (upper row) and $Al_{0.3}Ga_{0.7}Sb/InAs$-QWs (lower row). The momentum scattering was assumed to be isotropic (type I, see Table II) and independent of T.

$$J_1(\beta\mu_0) = E_F\beta. \tag{16b}$$

For arbitrary n, the integrals $J_n(\beta\mu_0)$ can be represented in closed form in terms of Lerch functions.[28] As this offers no advantage with respect to the numerical evaluation, we calculate $J_n(\beta\mu_0)$ by numerical quadrature.

The transport relaxation time τ_{tr} can be obtained from

$$\tau_{tr} = \frac{\int E\tau_1(E)\frac{\partial F_0}{\partial E}dE}{\int E\frac{\partial F_0}{\partial E}dE} = \frac{\hat{I}\Xi E^{\nu+1}}{\hat{I}E} = \frac{\Xi J_{\nu+1}(\beta\mu_0)}{\beta^{\nu+1}E_F}, \tag{17}$$

see Eq. (A4) in the Appendix. Using

$$\hat{I}\tau_1 E^i = \frac{\beta^{\nu+1}\tau_{tr}E_F\hat{I}E^{\nu+i}}{J_{\nu+1}(\beta\mu_0)} = \frac{\beta^{1-i}\tau_{tr}E_F}{1-e^{-E_F\beta}}\frac{J_{\nu+i}(\beta\mu_0)}{J_{\nu+1}(\beta\mu_0)} \tag{18}$$

where $i=1,2,3$, we simplify Eq. (5):

$$\frac{1}{\tau_z} = \frac{4}{\hbar^2}\frac{\beta E_F}{1-e^{-E_F\beta}}\tau_{tr}\left[(\alpha^2 + \gamma^2\langle k_z^2\rangle^2)\frac{\zeta}{\beta} \right.$$
$$-\frac{\gamma^2\langle k_z^2\rangle}{2}\left(\frac{\zeta}{\beta}\right)^2\frac{J_{\nu+2}(\beta\mu_0)}{J_{\nu+1}(\beta\mu_0)}$$
$$\left. +\gamma^2\frac{1+\tau_3/\tau_1}{16}\left(\frac{\zeta}{\beta}\right)^3\frac{J_{\nu+3}(\beta\mu_0)}{J_{\nu+1}(\beta\mu_0)}\right], \tag{19a}$$

$$\frac{1}{\tau_\pm} = \frac{2}{\hbar^2}\frac{\beta E_F}{1-e^{-E_F\beta}}\tau_{tr}\left[(\pm\alpha - \gamma\langle k_z^2\rangle)^2\frac{\zeta}{\beta} + \frac{\gamma}{2}(\pm\alpha - \gamma\langle k_z^2\rangle)\right.$$
$$\left.\times\left(\frac{\zeta}{\beta}\right)^2\frac{J_{\nu+2}(\beta\mu_0)}{J_{\nu+1}(\beta\mu_0)} + \gamma^2\frac{1+\tau_3/\tau_1}{16}\left(\frac{\zeta}{\beta}\right)^3\frac{J_{\nu+3}(\beta\mu_0)}{J_{\nu+1}(\beta\mu_0)}\right]. \tag{19b}$$

These formulas generalize the hitherto[13] known limiting cases of the low and high temperature regime of the DP spin relaxation in quasi-2D systems.

IV. NUMERICAL RESULTS

To illustrate the theory developed in the preceding section we show in Fig. 1 the spin relaxation rates τ_z^{-1} and $\tau_\pm^{-1}$ cal-

TABLE I. Measured carrier density n, Hall mobility μ_{Hall}, and spin-relaxation time τ_z of the samples investigated by Terauchi *et al.* (Ref. 20). The samples (a), (b), and (c) were n-doped in the barrier only, while (d), (e), and (f) were n-doped in the well only. The samples (g) and (h) were n- and (weakly) p-doped in the well. All values refer to room temperature.

Doping	Sample	n [10^{11} cm^{-2}]	μ_{Hall} [cm^2/V s]	τ_z [ps]
Barrier	(a)	1.4	4600	33
n-doped	(b)	2.6	4700	32
	(c)	4.7	4200	37
Well	(d)	0.4	3500	35
n-doped	(e)	2.4	2800	43
	(f)	6.0	2500	49
Well n- and	(g)	4.7	800	105
p-doped	(h)	9.8	1500	56

culated as a function of carrier density n and temperature T for asymmetric (001) grown AlGaAs/GaAs-QWs and AlGaSb/InAs-QWs with well width $L=100$ Å. The spin splitting was calculated self-consistently assuming that the samples were n-doped on one side only. We used $\tau_{tr}=0.1$ ps (Ref. 29) and we assumed that the momentum scattering was isotropic. The parameters are thus the same as in Ref. 12 so that our results for $T=1$ K reproduce the values obtained in Ref. 12 using the formulas for the low temperature limit of DP spin relaxation. At moderately high densities, the calculated rates usually increase with increasing temperature by less than an order of magnitude. In Fig. 1 we have assumed that τ_{tr} does not depend on T. In real systems, τ_{tr} can decrease by more than an order of magnitude for such an increase in temperature. Therefore we can usually expect smaller spin relaxation rates at room temperature as compared to low temperatures.

The largest variation of the spin-relaxation rates with temperature occurs in the low density range. Here, the thermal energy k_BT and the Fermi energy E_F are of the same order of magnitude for low T. On the other hand, at higher temperatures the spin relaxation is no longer controlled by E_F but by k_BT. This results in the pronounced temperature dependence at low densities which is visible in Fig. 1. The weaker temperature dependence obtained for the InAs-based systems in comparison with GaAs-based systems can be related to the term proportional to T^3 in Eq. (19), which dominates at low temperature for GaAs due to its larger effective mass m^* and smaller $\langle k_z^2 \rangle$.

The strong anisotropy of the spin-relaxation times, i.e., the difference between τ_+^{-1} and τ_-^{-1} and the nonmonotonous behavior[12] persist up to temperatures $T \sim 100$ K for the GaAs system and even far beyond room temperature for the InAs system. The huge difference, previously predicted for low temperature,[12] which is seen for densities around $n \sim 0.6 \times 10^{12}$ cm^{-2} in the systems considered here, is therefore remarkably stable with increasing temperature. For example,
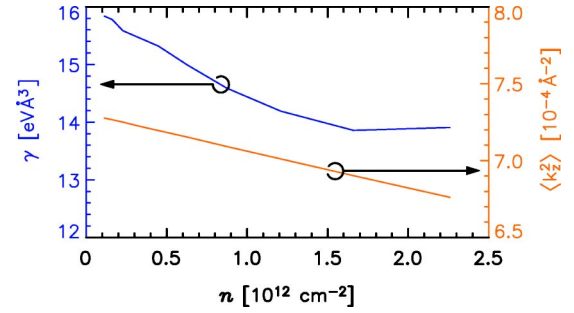

FIG. 2. (Color online) Calculated BIA spin splitting parameters γ (left axis) and $\langle k_z^2 \rangle$ (right axis) as a function of carrier density n for symmetrically doped Al$_{0.4}$Ga$_{0.6}$As/GaAs-QWs with $L=75$ Å.

the rate τ_-^{-1} in the InAs system at $n \sim 0.4 \times 10^{12}$ cm^{-2} is approximately 50 times smaller than τ_z^{-1} or τ_-^{-1} even at room temperature.

V. COMPARISON WITH ROOM TEMPERATURE EXPERIMENTS

Next, we calculate the spin-relaxation times τ_z of symmetrically n-doped (001)-grown QWs and compare our results with the experimental data obtained by Terauchi *et al.*[20] and Ohno *et al.*[21] In both experiments the authors used a pump-probe technique with circularly polarized light. The Al$_{0.4}$Ga$_{0.6}$As/GaAs QW had a width $L=75$ Å. The sample parameters and measured[30] τ_z for the eight samples investigated by Terauchi *et al.* are reproduced in Table I. For these systems we calculated the spin splitting and extracted the values of the BIA spin-splitting parameters γ and $\langle k_z^2 \rangle$ as a function of the carrier density n (see Fig. 2). The details of this procedure have been described in Ref. 12. Due to the symmetric doping of the samples, there is no Rashba effect and $\alpha=0$.

The spin-relaxation rates in Eq. (19) depend on the transport relaxation time τ_{tr} which is related to the transport mobility μ_{tr} via

$$\mu_{tr} = \frac{e\tau_{tr}}{m^*}. \tag{20}$$

Terauchi *et al.*[20] determined for their samples the Hall mobilities μ_{Hall}, see Table I. These Hall mobilities are equal to the transport mobilities only if the dominant scattering mechanisms are isotropic [i.e., $W(\mathbf{k}_\parallel, \mathbf{k}_\parallel')$ does not depend on the angle θ]. If small-angle scattering predominates the transport mobility μ_{tr} and the Hall mobility μ_{Hall} differ by the Hall factor r_{Hall}.[25] A more detailed discussion of the effects of various scattering mechanisms is given in the Appendix. For the samples investigated by Terauchi *et al.*,[20] the dominant scattering mechanisms were not known. Therefore we have considered three categories of scattering mechanisms listed in Table II and denoted as types I, II, and III. Calculated values of the Hall factor r_{Hall} are given in the same table.

Taking into account these effects and using the bulk GaAs effective mass ($m^*/m_0=0.0665$), we obtain the transport re-

TABLE II. Energy dependence, scattering angle characteristic, and Hall factor for various scattering mechanisms. We have listed the exponents for the power-law behavior of the momentum relaxation time [Eq. (13)] for bulk (Refs. 25, 27, 35, and 36) (ν^{3D}) and 2D systems (ν^{2D}) based on Eq. (A7). The scattering angle characteristic is specified by the ratio of the scattering times τ_3/τ_1 (cf. Sec. A 2). The Hall factor r_{Hall} is the ratio of Hall and transport mobility (cf. Sec. A 3).

		3D		2D		
	Scattering mechanism	ν^{3D}	r_{Hall}^{3D}	ν^{2D}	τ_3/τ_1	r_{Hall}^{2D}
Type I:	acoustic phonons (deformation potential) optical phonons (deformation potential) ionized impurities (screened) neutral impurities alloy scattering interface roughness	$-1/2$	$3\pi/8$	0	1	1
Type II:	acoustic phonons (polar, piezoelectric) optical phonons (polar)	$+1/2$	$45\pi/128$	1	$1/3$	$7/5$
Type III:	ionized impurities (weakly screened)	$+3/2$	$415\pi/512$	2	$1/9$	$99/35$

laxation time τ_{tr} from Eq. (20). For the samples in Table I the mobilities were measured only at room temperature. In order to derive the results shown in this section, we have thus used in Eq. (19) the same value of τ_{tr} for all temperatures. Accordingly, the temperature dependence of the spin-relaxation rates is determined only by the Fermi distribution. A different experiment, where this restriction does not apply, will be discussed below in Sec. VI.

The calculated results are shown in Fig. 3 together with the experimental data of Terauchi *et al.*. For comparison, we also show the results based on the formulas for the low and high temperature limit, respectively. It can be seen that Eq. (19) reproduces the results obtained with the simplified formulas for the corresponding limits. For most of the systems investigated by Terauchi *et al.*, room temperature falls into the nondegenerate (high temperature) limit. However, in the more heavily doped samples a significant deviation appears. For sample (h) the value of τ_z predicted by the theory for the nondegenerate limit is approximately 60% larger than the value obtained using Eq. (19).

In GaAs at room temperature, the mobility is limited by scattering at the deformation potential of acoustic phonons (type I) and at polar optical phonons (type II). The scattering at ionized impurities (weakly screened: type II; screened: type I), which usually dominates the mobility at low T, is not relevant here. Therefore the results calculated for scattering mechanisms of type III do not apply in the present case.

The experimental values for the spin relaxation time are between the theoretical results obtained for scattering mechanisms of type I and II. For the samples (g) and (h) the measured values are significantly closer to the theoretical values obtained for type I scattering than for all other samples. This agrees well with the fact that only these two samples were codoped with donors and acceptors. The scattering at neutral acceptors makes type I scattering more important for these

samples. This reasoning is supported by the fact that the samples (g) and (h) have the smallest mobilities (see Table II) which we attribute to the additional scattering mechanism.

In summary, we have achieved quantitative agreement between theory and experiment for the spin-relaxation rates of eight different samples. A similar EFA-based approach was applied by Lau *et al.*[14] for the samples discussed here with comparable results. However, the previous work did not take into account the doping self-consistently and no explicit formulas were given for the treatment of the temperature dependence of the spin relaxation. Furthermore, we would like to emphasize that it is important to take into account the difference between the Hall mobility usually measured in experiments and the transport mobility, which governs the spin relaxation. To the best of our knowledge, so far this aspect has not been taken into account in the context of spin relaxation.

VI. COMPARISON WITH TEMPERATURE-DEPENDENT MEASUREMENTS

The spin-relaxation time depends on the temperature via the Fermi distribution function and the variation of the transport mobility. To get a more detailed understanding of the interplay of these quantities we compare our theoretical results with the spin-relaxation times measured as a function of temperature by Ohno *et al.*[21] The sample used in their experiment corresponds to sample (d) of Table I. The measured values of the spin-relaxation time τ_z and the Hall mobility μ_{Hall} are reproduced in Fig. 4. Once again, the spin-relaxation time τ_z has been calculated as a function of temperature. But in contrast to Fig. 3, we have used here the temperature-dependent transport relaxation time obtained from the Hall mobility measured as a function of T. Figure
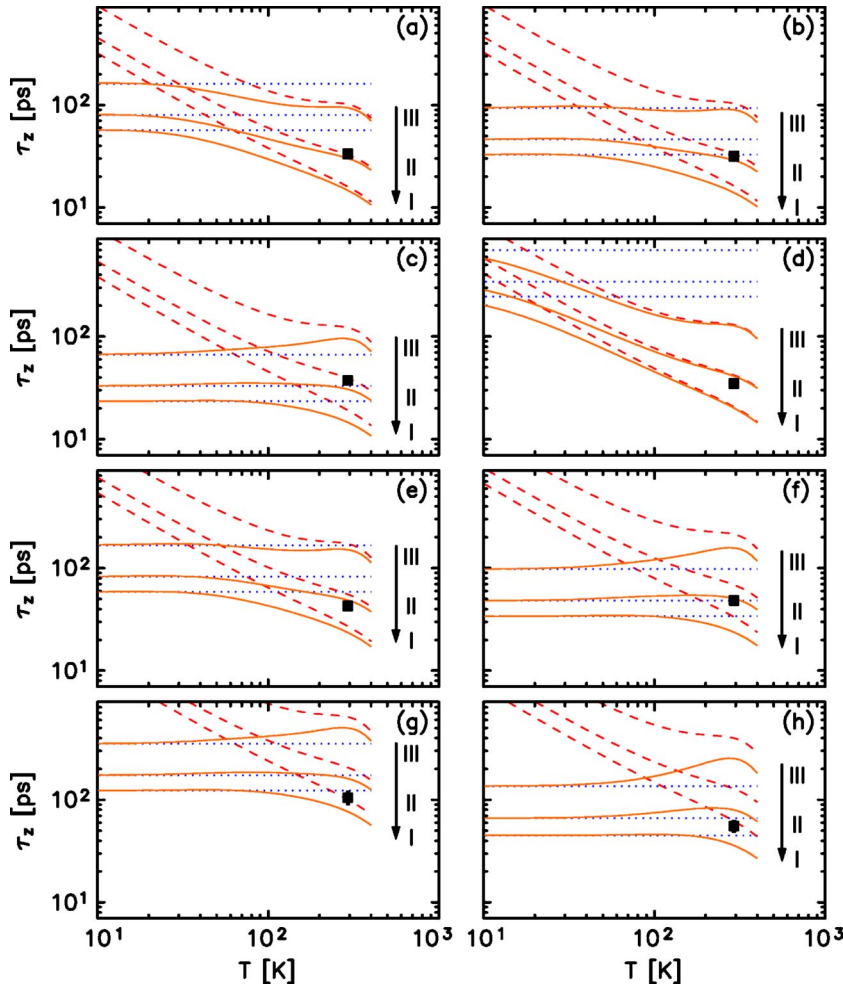
FIG. 3. (Color online) Calculated spin-relaxation time τ_z of different samples (a)–(h) as a function of temperature T in comparison with room temperature measurements (squares) from Terauchi et al. (Ref. 20). The theoretical results refer to the degenerate limit (dotted lines), to the nondegenerate limit (dashed lines), and to the generalized theory (full lines). For each set of curves, the upper curve corresponds to scattering at weakly screened ionized impurities (type III), while the middle and lower curves represent momentum scattering of types II and I, respectively (see Table II).

4(a) shows the theoretical results of the extended theory for the three types of scattering mechanisms together with the results assuming the degenerate and nondegenerate limit.

Once again, an excellent quantitative agreement between theory and experiment can be achieved at room temperature assuming that the dominant scattering mechanisms are of type II (e.g., polar optical phonons). The measured decrease of the Hall mobility at high temperatures is a signature of phonon scattering,[25] which agrees well with this interpretation.

In the low temperature range (up to about 100 K) the experimental data are well explained by type III scattering (i.e., by scattering at weakly screened impurities). In samples which are not modulation doped, like the ones considered here, this scattering mechanism usually limits the mobility at low temperatures and leads to a characteristic increase of the mobility with increasing temperature [Fig. 4(b)].

The temperature dependence of the Hall mobility at intermediate temperatures ($80~\mathrm{K} \lesssim T \lesssim 200~\mathrm{K}$) indicates that ionized impurity scattering becomes less important with increasing temperature. Instead, phonon scattering becomes the dominant scattering mechanism. As expected, the measured values of $\tau_z(T)$ depart from the calculated curve for type III scattering with increasing temperature and approach the curve for type II scattering (polar phonon scattering). While we have a remarkably good agreement between theory and

experiment for $T \gtrsim 20~\mathrm{K}$, a discrepancy arises at low temperatures $T \lesssim 20~\mathrm{K}$. As the Hall mobility was not measured for $T < 13~\mathrm{K}$ this deviation cannot be examined more closely. It could be caused by approximations in the scattering theory. For example, at low temperatures the simple power-law dependence in Eq. (13) becomes incorrect for ionized impurity scattering.[25] In samples with high mobilities (mobilities larger than the mobilities of the samples studied in this work) the electron-electron collisions neglected here constitute a further possible source of systematic errors. Such processes conserve the total momentum of the electron system so that they do not affect the mobility. The DP spin relaxation, on the other hand, is reduced by any kind of scattering. We therefore have a correction due to electron-electron scattering, which is particularly important in high mobility samples.[22,32,33] Finally, it is possible that in the pump-probe experiment by Ohno et al.[21] the laser beam heated up the electron system so that the electron temperature was indeed higher than shown in Fig. 4(a).[34]

VII. CONCLUSIONS

Based on the self-consistent multiband envelope function approximation, we obtain an accurate description of the spin splitting and Dyakonov-Perel spin relaxation in quasi-2D systems. In the present work, we extend the theory of DP
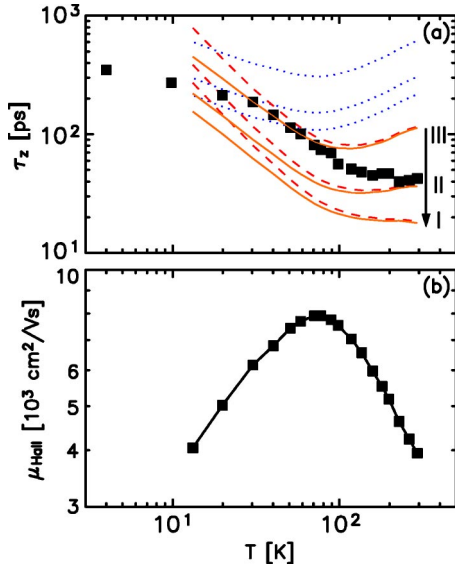
FIG. 4. (Color online) (a) Spin-relaxation time τ_z and (b) measured (Refs. 21 and 31) Hall mobility μ_{Hall} as a function of temperature T. In (a) the labeling of the calculated curves is analogous to Fig. 3 and the measured values (Ref. 21) are represented by squares. The sample parameters are those of sample (d) in Table I. In the very low temperature range $T < 13$ K, no theoretical evaluation of τ_z is possible due to lack of experimental data for the Hall mobility.

spin relaxation in order to connect the previously known results for the limiting cases of low and high temperatures. Therefore our realistic theory renders considerations with respect to the degeneracy or nondegeneracy of the electron system unnecessary.

We demonstrate the strengths of our approach by comparing with spin-relaxation times τ_z measured by Terauchi *et al.*[20] and Ohno *et al.*[21] for a large variety of different samples. Using a simple model,[9] the latter authors obtained theoretical estimates for τ_z that differed by an order of magnitude from the experimental values, whereas we are able to obtain excellent quantitative agreement between experiment and theory.

Up to now, the spin-relaxation times $\tau_{\pm}$ could not be determined experimentally. We corroborate here the prediction[11,12] that one of the times τ_+ or τ_- increases nonmonotonously as a function of electron density. Our temperature-dependent calculations show that this feature is remarkably stable with increasing temperature and that it is connected with a huge anisotropy of the spin relaxation.

ACKNOWLEDGMENTS

APPENDIX: SCATTERING THEORY

In this appendix we give a short overview of the energy dependence and scattering angle characteristic of various electron momentum scattering mechanisms. As commonly done in the literature,[25,27,35–37] we assume that the electron system is nondegenerate and that the scattering is quasielastic, i.e., the scattering does not change the kinetic energy. We start by considering bulk systems. Then we discuss the modifications necessary for 2D systems.

1. Relaxation times

In this work we treat scattering based on Fermi's golden rule, where the transition rate $W(\boldsymbol{k},\boldsymbol{k}')$ between states with wave vectors $\boldsymbol{k}$ and $\boldsymbol{k}'$ is[25]

$$W(\boldsymbol{k},\boldsymbol{k}') = \frac{2\pi}{\hbar}|H^{\text{scatt}}_{\boldsymbol{k}'\boldsymbol{k}}|^2 \delta[E(\boldsymbol{k}') - E(\boldsymbol{k})], \tag{A1a}$$

$$H^{\text{scatt}}_{\boldsymbol{k}'\boldsymbol{k}} = \frac{1}{\Omega}\int_{\Omega} e^{-i\boldsymbol{k}'\cdot\boldsymbol{r}} U^{\text{scatt}}(\boldsymbol{r}) e^{i\boldsymbol{k}\cdot\boldsymbol{r}} d^3 r \tag{A1b}$$

with the crystal volume Ω and the scattering potential $U^{\text{scatt}}(\boldsymbol{r})$. Using the effective mass approximation (9), we obtain for the scattering rate out of the state $|\boldsymbol{k}\rangle$ into any other state $|\boldsymbol{k}'\rangle$ of a nondegenerate electron system[25]

$$\frac{1}{\tau(\boldsymbol{k})} = \overset{\sim}{\sum_{\boldsymbol{k}'}} W(\boldsymbol{k},\boldsymbol{k}'). \tag{A2}$$

Here the tilde indicates that the sum is restricted to final states $|\boldsymbol{k}'\rangle$ with the same spin orientation as the initial state, i.e., we have assumed that the scattering processes do not change the spin. The scattering time $\tau(\boldsymbol{k})$ is the average time between scattering events, i.e., it can be identified with the time during which the electron is in the state $|\boldsymbol{k}\rangle$.

For nonisotropic scattering mechanisms the information about the initial momentum is not lost after the time $\tau(\boldsymbol{k})$, but decays on the time scale of the momentum relaxation time $\tau_1(\boldsymbol{k})$, which is defined as[25]

$$\frac{1}{\tau_1(\boldsymbol{k})} = \overset{\sim}{\sum_{\boldsymbol{k}'}} W(\boldsymbol{k},\boldsymbol{k}')(1 - \cos\theta). \tag{A3}$$

For elastic scattering, as assumed here, $\tau_1(\boldsymbol{k})$ depends only on the energy $E(\boldsymbol{k})$ (see Sec. A 2). The time τ_1 determines the transport mobility via Eq. (20) and[13,25]

$$\tau_{\text{tr}} = \frac{\displaystyle\int dE Z(E) E \frac{\partial F_0}{\partial E} \tau_1(E)}{\displaystyle\int dE Z(E) E \frac{\partial F_0}{\partial E}}. \tag{A4}$$

Here, F_0 is the Fermi distribution function (11). Assuming a parabolic dispersion (9), the density of states $Z(E)$ is proportional to $\sqrt{E}$ in 3D systems and it is independent of E in 2D systems.

2. Scattering angle characteristic

In the framework of the aforementioned approximations, the transition rate $W(\boldsymbol{k},\boldsymbol{k}')$ can be expressed for many scattering mechanisms as a power law[35]

$$W(\boldsymbol{k},\boldsymbol{k}') \propto \frac{1}{q^{2\nu}}, \tag{A5}$$

where q is the momentum transfer

$$q \equiv |\boldsymbol{k} - \boldsymbol{k}'| = 2k \sin(\theta/2) \tag{A6a}$$

$$= 2\sqrt{\zeta E} \sin(\theta/2). \tag{A6b}$$

Combining these equations with Eq. (8) we get Eq. (13). In Table II we have compiled from the literature[25,27,35,36] the exponents ν for various scattering mechanisms. The scattering mechanisms of type I are isotropic, while for types II and III small angle scattering is increasingly predominant. The values of ν for 2D systems are derived from the values for 3D systems, using the fact that the momentum scattering rates $1/\tau_1$ are proportional to the density of states.[25] Assuming that the remaining contributions to the exponent ν do not depend on the dimensionality of the system, we thus have

$$\nu^{2D} = \nu^{3D} + 1/2. \tag{A7}$$

For some scattering mechanisms, values of ν^{2D} have been given explicitly in the literature.[38,39] They agree with our values in Table II.

Using Eqs. (8), (A5), and (A6) we have in 2D systems

$$\frac{1}{\tau_n} \propto \int_0^{2\pi} d\theta \, \frac{1 - \cos(n\theta)}{\sin^{2\nu}(\theta/2)}. \tag{A8}$$

Thus we get[40]

$$\frac{\tau_3}{\tau_1} = \begin{cases} \dfrac{(2-\nu)(3-\nu)}{\nu^2 - \nu + 6}, & \nu \leq 3/2 \\[2mm] 1/9, & \nu > 3/2. \end{cases} \tag{A9}$$

The values for the ratio τ_3/τ_1 obtained by means of Eq. (A9) are listed in Table II. They are identical with the values used by Lau *et al.*[14] as far as they are given there.

3. Hall and transport mobility

In general, the mobility μ_{Hall} determined from Hall measurements differs from the transport mobility μ_{tr} (obtained from, e.g., the experimental conductance) by the Hall factor[25,27]

$$r_{\text{Hall}} = \frac{\mu_{\text{Hall}}}{\mu_{\text{tr}}}. \tag{A10}$$

The values of r_{Hall} in Table II have been obtained from the exponent ν (for 3D and 2D systems, respectively) using[25,27]

$$r_{\text{Hall}} = \frac{\Gamma(2\nu + 5/2)\Gamma(5/2)}{[\Gamma(\nu + 5/2)]^2}, \tag{A11}$$

where Γ denotes the gamma function.[28] We have $1 \leq r_{\text{Hall}} \leq 99/35$, i.e., $\mu_{\text{tr}} \leq \mu_{\text{Hall}}$.

*Electronic address: josef.kainz@physik.uni-regensburg.de

[1] D. P. DiVincenzo, Science **270**, 255 (1995).

[2] G. A. Prinz, Science **282**, 1660 (1998).

[3] S. A. Wolf, D. D. Awschalom, R. A. Buhrman, J. M. Daughton, S. von Molnár, M. L. Roukes, A. Y. Chtchelkanova, and D. M. Treger, Science **294**, 1488 (2001).

[4] *Semiconductor Spintronics and Quantum Computations*, edited by D. D. Awschalom, D. Loss, and N. Samarth (Springer, Berlin, 2002).

[5] M. Oestreich, M. Bender, J. Hübner, D. Hägele, W. W. Rühle, T. Hartmann, P. J. Klar, W. Heimbrodt, M. Lampalzer, K. Volz, and W. Stolz, Semicond. Sci. Technol. **17**, 285 (2002).

[6] G. E. Pikus and A. N. Titkov, in *Optical Orientation*, edited by F. Meier and B. P. Zakharchenya (Elsevier, Amsterdam, 1984), Chap. 3, pp. 73–131.

[7] M. I. Dyakonov and V. I. Perel, Sov. Phys. JETP **33**, 1053 (1971) [Zh. Eksp. Teor. Fiz. **60**, 1954 (1971)].

[8] M. I. Dyakonov and V. I. Perel, Sov. Phys. Solid State **13**, 3023 (1972) [Fiz. Tverd. Tela (Leningrad) **13**, 3581 (1971)].

[9] M. I. Dyakonov and V. Y. Kachorovskii, Sov. Phys. Semicond. **20**, 110 (1986) [Fiz. Tekh. Poluprovodn. (S.-Peterburg) **20**, 178 (1986)].

[10] N. S. Averkiev, L. E. Golub, and M. Willander, J. Phys.: Condens. Matter **14**, R271 (2002).

[11] N. S. Averkiev and L. E. Golub, Phys. Rev. B **60**, 15 582 (1999).

[12] J. Kainz, U. Rössler, and R. Winkler, Phys. Rev. B **68**, 075322 (2003).

[13] N. S. Averkiev, L. E. Golub, and M. Willander, Sov. Phys. Semicond. **36**, 91 (2002) [Fiz. Tekh. Poluprovodn. (S.-Peterburg) **36**, 97 (2002)].

[14] W. H. Lau, J. T. Olesberg, and M. E. Flatté, Phys. Rev. B **64**, 161301(R) (2001).

[15] G. L. Bir, A. G. Aronov, and G. E. Pikus, Sov. Phys. JETP **42**, 705 (1976) [Zh. Eksp. Teor. Fiz. **69**, 1382 (1975)].

[16] G. Dresselhaus, Phys. Rev. **100**, 580 (1955).

[17] Y. A. Bychkov and E. I. Rashba, J. Phys. C **17**, 6039 (1984).

[18] J. Rudolph, D. Hägele, H. M. Gibbs, G. Kithrova, and M. Oestreich, Appl. Phys. Lett. **82**, 4516 (2003).

[19] R. Winkler and U. Rössler, Phys. Rev. B **48**, 8918 (1993).

[20] R. Terauchi, Y. Ohno, T. Adachi, A. Sato, F. Matsukara, A. Tackeuchi, and H. Ohno, Jpn. J. Appl. Phys., Part 1 **38**, 2549 (1999).

[21] Y. Ohno, R. Terauchi, T. Adachi, F. Matsukura, and H. Ohno, Physica E (Amsterdam) **6**, 817 (2000).

[22] M. M. Glazov and E. L. Ivchenko, JETP Lett. **75**, 403 (2002) [Pis'ma Zh. Eksp. Teor. Fiz. **75**, 476 (2002)].

[23] M. A. Brand, A. Malinowski, O. Z. Karimov, P. A. Marsden, R. T. Harley, A. J. Shields, D. Sanvitto, D. A. Ritchie, and M. Y. Simmons, Phys. Rev. Lett. **89**, 236601 (2002).

[24] M. Braun and U. Rössler, J. Phys. C **18**, 3365 (1985).

[25] M. Lundstrom, *Fundamentals of Carrier Transport*, 2nd ed.

(Cambridge University Press, Cambridge, England, 2000).

[26] This condition is fulfilled if $\Delta\mu \ll k_B T$ or if $\Delta\mu \ll E_F$. In the latter case, $\hat{I}$ may only be applied to terms E^ν with exponents $\nu \geq 1$ and with $(\Delta\mu)^2 \ll 24 E_F^2/[\nu(\nu-1)]$.

[27] J. Singh, *Physics of Semiconductors and Their Heterostructures* (McGraw-Hill, New York, 1993).

[28] I. S. Gradshteyn and I. M. Ryzhik, *Table of Integrals, Series and Products* (Academic, San Francisco, 1996).

[29] Note that all rates are proportional to τ_{tr} and can therefore be easily rescaled, e.g., to match measured values of τ_{tr}.

[30] Due to different definitions of the spin-relaxation time the values given here differ from those in Ref. 20 by a factor of 2.

[31] Y. Ohno (private communication, 2003).

[32] M. M. Glazov, Sov. Phys. Solid State **45**, 1162 (2003) [Fiz. Tverd. Tela (Leningrad) **45**, 1108 (2003)].

[33] M. M. Glazov, E. L. Ivchenko, M. A. Brand, O. Z. Karimov, and R. T. Harley, *11th International Symposium "Nanostructures: Physics and Technology,"* edited by Zh. Alferov and L. Esaki, Ioffe Physico-Technical Institute, St. Petersburg, 2003, p. 273.

[34] M. Oestreich (private communication, 2004).

[35] V. F. Gantmakher and Y. B. Levinson, *Carrier Scattering in Metals and Semiconductors* (North-Holland, Amsterdam, 1987).

[36] B. K. Ridley, *Quantum Processes in Semiconductors* (Clarendon, Oxford, 1993).

[37] R. Ferreira and G. Bastard, Phys. Rev. B **40**, 1074 (1989).

[38] K. Hess, Appl. Phys. Lett. **35**, 484 (1979).

[39] K. Lee, M. S. Shur, T. J. Drummond, and H. Morkoç, J. Appl. Phys. **54**, 6432 (1983).

[40] F. G. Pikus and G. E. Pikus, Phys. Rev. B **51**, 16 928 (1995).